

Synthesis, Characterization, and Molecular Orbital Analysis of $[\text{Et}_4\text{N}]_2[(\text{OC})_5\text{MoAsMo}_3(\text{CO})_9(\mu_3\text{-OR})_3\text{Mo}(\text{CO})_3]$ (R = Me, Et). X-ray Structure of $[\text{Et}_4\text{N}]_2[(\text{OC})_5\text{MoAsMo}_3(\text{CO})_9(\mu_3\text{-OMe})_3\text{Mo}(\text{CO})_3]\cdot 0.6\text{thf}$

Jaap W. van Hal,[†] Kenton H. Whitmire,^{*,†} Bachir Zouhoune,^{*,§} Jean-François Halet,[‡] and Jean-Yves Saillard^{*,‡}

Department of Chemistry, Rice University, P.O. Box 1892, Houston, Texas 77251, and Laboratoire de Chimie du Solide et Inorganique Moléculaire, URA CNRS 1495, Université de Rennes I, 35042 Rennes Cedex, France

Received October 13, 1994[Ⓢ]

NaAsO_2 reacts with $\text{Mo}(\text{CO})_6$ in refluxing methanol or ethanol to yield $[\text{Et}_4\text{N}]_2[(\text{OC})_5\text{MoAsMo}_3(\text{CO})_9(\mu_3\text{-OR})_3\text{Mo}(\text{CO})_3]$ (R = Me, $[\text{Et}_4\text{N}]_2[\text{Ia}]$; R = Et, $[\text{Et}_4\text{N}]_2[\text{Ib}]$). The compound $[\text{Et}_4\text{N}]_2[\text{Ia}]$ crystallizes as the thf solvate, $[\text{Et}_4\text{N}]_2[\text{Ia}]\cdot 0.6\text{thf}$, in space group $P2_1/n$, with $a = 12.0420(46)$ Å, $b = 25.7455(81)$ Å, $c = 18.1991(56)$ Å, $\beta = 94.277(28)^\circ$, and $V = 5626(5.9)$ Å³, and was refined on F^2 to $wR2 = 0.1802$ and a conventional $R1 = 0.0836$. The anion $[\text{Ia}]^{2-}$ is built around a tetrahedral AsMo_3 core. A $\text{Mo}(\text{CO})_3$ fragment is bonded to the Mo_3 base via three triply bridging methoxy ligands. The structure is completed by a $\text{Mo}(\text{CO})_5$ fragment which is bonded to the lone pair of the As. The compound does not obey the usual electron-counting rules, and extended Hückel calculations on an idealized model with C_{3v} symmetry showed that the extra electron pair is located in an a_2 orbital, equally delocalized over the three molybdenum atoms of the Mo_3 base.

Introduction

The interaction between hydroxy and alkoxy ligands and group 6 metal carbonyl compounds has been studied intensively, not only because of their interesting metal to metal interactions but also because of their ability to catalyze the water gas shift reaction as well as hydrogenation of aldehydes and ketones.¹ The first systematic research in this system is described in a series of papers by Hieber and co-workers,² who reacted KOH and $\text{M}(\text{CO})_6$ (M = Cr, Mo, W) in protic solvents. Since then, several polynuclear alkoxide/hydroxide compounds have been synthesized and structurally characterized, such as $[\text{Mo}(\text{OH})(\text{CO})_2(\text{NO})]_4$,³ $[\text{W}(\text{OH})(\text{CO})_3\text{H}]_4$ (Hieber's Acid),⁴ $[\text{Et}_4\text{N}]_3[\text{W}_2(\text{CO})_6(\text{O}^-\text{Ph})_3]$,⁵ $[\text{Et}_4\text{N}]_n[\text{M}(\text{OR})(\text{CO})_3]_n$ ($n = 3, 4$; M = Cr, Mo, W; R = H, Me, Et, Ph).^{6,7} It was also found that compounds of the form $\text{M}(\text{CO})_5(\text{OR})^-$ will react reversibly with CO_2 to form $\text{M}(\text{CO})_5(\text{O}_2\text{COR})^-$, and the structure of $[\text{W}(\text{CO})_5\text{O}_2\text{COH}]^-$ ⁸ was recently elucidated.

Compared to the other transition metal–heavy main group element compounds, arsenic-containing compounds are rare and

most of those reported to date are neutral. The series of heterometallic compounds $\{\text{MnCp}'(\text{CO})_2\}_2\text{AsMoCp}(\text{CO})_2$ and $\{\text{Cr}(\text{CO})_5\}_2\text{AsMCp}(\text{CO})_2$ (M = Mo, W)⁹ was synthesized from $\text{ClAs}(\text{Cr}(\text{CO})_5)_2$ or $\text{ClAs}(\text{MnCp}(\text{CO})_2)_2$ and $[\text{MCp}(\text{CO})_2]^-$ (M = Mo, W). Another series including $\text{As}_5\{\text{CpMo}\}_2$,¹⁰ $(\text{Cp}^*)_2\text{Mo}_2(\text{CO})_4\text{As}_2$, $(\text{Cp}^*)\text{Mo}(\text{CO})_2(\text{As}_3)$, $\text{As}\{\text{MoCp}(\text{CO})_2\}_3$,¹¹ and $\{\text{Cp}'\text{Mo}(\text{CO})_2\}_2(\text{As}_2)$ ¹² was created by treating $\{\text{CpMo}(\text{CO})_n\}_2$ ($n = 2, 3$) directly with arsines or arsenic metal. Iron– or cobalt–arsenic cluster carbonyl compounds are also known, among which are $\text{As}_2\text{Fe}_3(\text{CO})_9$,¹³ $\text{Fe}_2(\text{CO})_8\text{AsFe}_2(\text{CO})_6\text{Cl}$,¹⁴ $\text{Fe}_3(\text{CO})_9(\mu_3\text{-SR})(\mu_2\text{-AsR}'_2)$ (R = $t\text{-C}_4\text{H}_9$, C_6H_{11} ; R' = alkyl, aryl),¹⁵ $\text{Fe}_3(\text{CO})_9(\mu_3\text{-As})(\mu_3\text{-CH})$, $\text{Fe}_3(\text{CO})_9(\mu_3\text{CH})\{\mu_3\text{-AsCr}(\text{CO})_5\}$,¹⁶ $[\text{Fe}_2(\text{CO})_8(\mu_4\text{-As})]_2[\text{Fe}_2(\text{CO})_6]$, and $[\mu_4\text{-AsCo}_3(\text{CO})_8]_3$.¹⁷ Recently, the syntheses of $[\text{HAS}\{\text{Fe}(\text{CO})_4\}_3]^{2-}$ and $[\{\mu\text{-AsFe}(\text{CO})_4\}_2]^{2-}$ were reported.¹⁸

There are fewer compounds which incorporate main group elements as well as hydroxy/alkoxy ligands. Those known include $[(\text{As}(\text{O})_3(\text{CpMo})_3)]$, $[\text{As}(\text{O})_2(\text{S})\{\text{CpMo}\}_3]$,¹⁹ and Fe_2W_2

[†] Rice University.

[‡] Université de Rennes I.

[§] Permanent address: Institut de Chimie, Département de Chimie Inorganique, Université de Constantine, Constantine, Route de Aïn-el-Bey, Algeria.

[Ⓢ] Abstract published in *Advance ACS Abstracts*, October 1, 1995.

- Darensbourg, D. J.; Sanchez, K. M.; Reibenspies, J. H.; Rheingold, A. L. *J. Am. Chem. Soc.* **1989**, *111*, 7094–7103.
- Hieber, W.; Rieger, K. *Z. Anorg. Allg. Chem.* **1959**, *300*, 288–294. Hieber, W.; Eglert, K.; Rieger, K. *Z. Anorg. Allg. Chem.* **1959**, *300*, 295–303. Hieber, W.; Eglert, K.; Rieger, K. *Z. Anorg. Allg. Chem.* **1959**, *300*, 304–310.
- Albano, V.; Bellon, P.; Ciani, G.; Manassero, M. *J. Chem. Soc., Chem. Commun.* **1969**, 1242–1243.
- Albano, V. G.; Ciani, G.; Manassero, M.; Sansoni, M. *J. Organomet. Chem.* **1972**, *34*, 353–365.
- Darensbourg, D. J.; Sanchez, K. M.; Reibenspies, J. H. *Inorg. Chem.* **1988**, *27*, 3269–3270.
- Ellis, J. E.; Rochfort, G. L. *Organometallics* **1982**, *1*, 682–689.
- Mcneese, T. J.; Cohen, M. B.; Foxman, B. M. *Organometallics* **1984**, *3*, 552–556. McNeese, T. J.; Mueller, T. E.; Wierda, D. A.; Darensbourg, D. A.; Delord, T. *J. Inorg. Chem.* **1985**, *24*, 3465–3468. Lin, J. T.; Yeh, S. K.; Lee, G. H.; Wang, Y. *J. Organomet. Chem.* **1989**, *361*, 89–99.
- Darensbourg, D. J.; Meckfessel Jones, M. L.; Reibenspies, J. H. *Inorg. Chem.* **1993**, *32*, 4675–4676.

- Huttner, G.; Sigwarth, B.; von Siegel, J.; Zsolnai, L. *Chem. Ber.* **1982**, *115*, 2035–2043.
- Rheingold, A. L.; Foley, M. J.; Sullivan, P. J. *J. Am. Chem. Soc.* **1982**, *104*, 4277–4279.
- Bernal, I.; Brunner, H.; Meier, M.; Pfisterer, H.; Wachter, J.; Ziegler, M. L. *Angew. Chem., Int. Ed. Engl.* **1984**, *23*, 438–439. Blechsmitt, K.; Pfisterer, K.; Zahn, T.; Ziegler, M. L. *Angew. Chem., Int. Ed. Engl.* **1985**, *24*, 66–67. Ziegler, M. L.; Blechsmitt, K.; Nuber, B.; Zahn, T. *Chem. Ber.* **1988**, *121*, 159–171.
- Di Maio, A.-J.; Rheingold, A. L. *J. Chem. Soc., Chem. Commun.* **1987**, 404–405.
- Delbaere, L. Y. J.; Kruczynski, L. J.; McBride, D. W. *J. Chem. Soc., Dalton Trans.* **1973**, 307–310.
- Huttner, G.; Mohr, G.; Pritzlaff, B.; von Seyerl, J.; Zsolnai, L. *Chem. Ber.* **1982**, *115*, 2044–2049.
- Winter, A.; Zsolnai, L.; Huttner, G. *J. Organomet. Chem.* **1983**, *250*, 409–429.
- Caballero, C.; Nuber, B.; Ziegler, M. L. *J. Organomet. Chem.* **1990**, *386*, 209–223.
- Arnold, L. J.; Mackey, K. M.; Nicholson, B. K. *J. Organomet. Chem.* **1990**, *387*, 197–207.
- Bachman, R. E.; Miller, S. K.; Whitmire, K. H. *Inorg. Chem.* **1994**, *33*, 2075–2076. Henderson, P.; Rossignoli, M.; Burns, R. C.; Scudder, M. L.; Craig, D. C. *J. Chem. Soc., Dalton Trans.* **1994**, 1641–1647. Bachman, R. E.; Whitmire, K. H. *Organometallics* **1995**, *14*, 796–803.

(μ_3 -S)₂(O-*i*-Pr)₆(CO)₅(py).²⁰ Recently, the compound [Et₄N]₂-[BiMo₄(CO)₁₂(μ_3 -OMe)₃]²¹ ([Et₄N]₂[II]) was synthesized from NaBiO₃ and Mo(CO)₆. We now wish to report the synthesis and structure as well as a detailed bonding analysis of the first anionic arsenic- and molybdenum-containing carbonyl compounds: [Et₄N]₂[(OC)₅MoAsMo₃(CO)₉(μ_3 -OR)₃Mo(CO)₃], where R = Me ([Et₄N]₂[Ia]) and R = Et ([Et₄N]₂[Ib]).

Experimental Section

General Methods. Unless otherwise specified, all synthetic manipulations were performed either with a vacuum line or under an atmosphere of purified nitrogen by employing standard drybox or Schlenk-type inert-atmosphere techniques. All solvents were distilled under nitrogen from the appropriate drying agents. Infrared spectra were obtained in 0.1 mm CaF₂ cells by using a Perkin-Elmer 1640 Fourier transform infrared spectrometer. Other reagents, such as [Et₄N]-Br, Mo(CO)₆, and NaAsO₂, were used as obtained from commercial sources. NMR spectra were recorded on a Bruker AF 300, operating at 300 MHz for ¹H and 75 MHz for ¹³C. Elemental analysis was performed in house using the Carlo Erba Instruments NA 1500 Series 2 analyzer. FAB mass spectra were obtained on a VG Analytical Autospec 3. Visible spectra were obtained on a Beckman DU 64 spectrophotometer.

Synthesis of [Et₄N]₂[Ia]. A Schlenk flask was charged with 1.0 mmol of NaAsO₂ (0.13 g) and 5.0 mmol of Mo(CO)₆ (1.3 g). To this were added 50 mL of MeOH and 5 mL of heptanes. The heptanes were added to rinse the Mo(CO)₆, which sublimes into the condenser, back into the reaction mixture. The mixture was sparged with dry dinitrogen for 30 min and refluxed overnight. The crude reaction mixture was filtered through a short column of Celite, and the filtrate was concentrated *in vacuo* to half its volume. Solid [Et₄N]Br (2.2 g, 10 mmol) was added, and the product was precipitated by adding twice the volume of deoxygenated water. The product was filtered off, washed with diethyl ether, dried *in vacuo*, and recrystallized from thf/hexanes (yield 0.7 g, 55%). Single crystals were obtained by slow diffusion at room temperature of hexanes into a thf solution of the products. The product is soluble in most polar organic solvents. IR (thf), cm⁻¹: 2071 m, 1966 vs, 1926 m, 1896 m, 1868 w. NMR, ppm: ¹H (CD₃CN), 3.883 (OMe), 1.201 (N(CH₂CH₃)₄⁺, t), 3.319 (N(CH₂CH₃)₄⁺, q); ¹³C (CD₃CN), 234.3, 229.58, 223.85, 217.01, 205.34 (carbonyl groups), 81.456 (OMe), 53.001 (N(CH₂CH₃)₄⁺), 7.586 (N(CH₂CH₃)₄⁺). Owing to the presence of lattice solvent, the sample for analysis was prepared by careful recrystallization and drying under vacuum for a week. Anal. Calcd (found) for C₃₆H₄₉As₁Mo₅N₂O₂₀: C, 31.23 (29.32); H, 3.57 (4.65); N, 2.02 (2.18). Numerous repeated attempts to obtain better C analyses were not successful despite use of carefully purified single crystals. FAB MS (positive ion, electrospray in CH₃CN, resolution 1000): *m/z* 1514 ([Et₄N]₃[Ia]⁺). UV-vis (MeCN): λ_{\max} = 355 nm, ϵ = 3 × 10⁴ M⁻¹ cm⁻¹; very weak shoulder at 475 nm.

Synthesis of [Et₄N]₂[Ib]. This compound was synthesized in a similar manner by using dry ethanol instead of methanol. It was purified by extracting the cluster into thf and allowing diethyl ether to diffuse slowly into the thf solution. Yield = 0.6 g (43%) of black needles. A second molybdenum compound, which contained no carbonyl stretches in the IR, was also obtained but was not further analyzed. IR (thf), cm⁻¹: 2068 m, 1965 vs, 1923 s, 1896 s, 1867 w. NMR: ¹H (CD₃CN), 3.766 (q, OCH₂CH₃), 1.485 (t, OCH₂CH₃), 3.148 (q, N(CH₂CH₃)₄⁺), 1.117 (t, N(CH₂CH₃)₄⁺); ¹³C, 233.18, 230.01, 224.15, 223.13, 218.05, 205.55 (carbonyl groups), 95.704 (OCH₂CH₃), 21.514 (OCH₂CH₃), 53.309 (N(CH₂CH₃)₄⁺), 7.997 (N(CH₂CH₃)₄⁺). NMR indicated the presence of approximately 0.5 thf per molecule even in well-dried crystals. Anal. Calcd (found) for C₃₉H₅₅AsMo₅N₂O₂₀:

Table 1. Crystal Data Collection and Refinement Parameters

empirical formula	C _{38.40} H _{53.80} AsMo ₅ N ₂ O _{20.60}
fw	1427.65
space group	P2 ₁ /n (No. 14)
<i>a</i> , Å	12.0420(46)
<i>b</i> , Å	25.7455(81)
<i>c</i> , Å	18.1991(56)
β , deg	94.277(28)
<i>V</i> , Å ³	5626(5.9)
<i>Z</i>	4
density (calcd), Mg/m ³	1.685
μ (Mo K α), mm ⁻¹	1.735
temp, K	213
radiation; λ , Å	Mo K α ; 0.7107
final <i>R</i> indices [<i>I</i> > 2 σ (<i>I</i>)] ^a	R1 = 0.0836, wR2 = 0.1802
<i>R</i> indices (all data) ^a	R1 = 0.1892, wR2 = 0.2496
transm coeff	0.71–1.00

^a R1 = $\sum ||F_o| - |F_c|| / \sum |F_o|$, wR2 = $[\sum [w(F_o^2 - F_c^2)^2] / \sum [w(F_o^2)^2]]^{0.5}$; $w = 1/[\sigma^2(F_o^2) + (0.0497P)^2 + 129.8741P]$; $P = (F_o^2 + 2F_c^2)/3$.

0.5C₄H₈O: C, 33.67 (33.90); H, 4.07 (3.80); N, 1.92 (1.87). UV-vis (MeCN): λ_{\max} = 390 nm, ϵ = 9 × 10³ M⁻¹ cm⁻¹; weak shoulder at 470 nm.

X-ray Crystallography. A needle-shaped black crystal of [Et₄N]₂[Ia] was cut to the dimensions 0.2 × 0.2 × 0.5 mm³, mounted on the tip of a glass fiber with epoxy cement, and immediately transferred to the cold stream on a Rigaku AFC5S automated single-crystal diffractometer. The unit cell was determined with 25 randomly selected reflections with 2 θ between 7 and 15°. Data were collected with the TEXSAN²² software package and were corrected for Lorentz-polarization effects and absorption (ψ scans, transmission range 0.71–1.00). Data collection and refinement parameters are summarized in Table 1. Scattering factors were taken from the literature.²³ Direct methods (SHELXS-86)^{24a} revealed the positions of the heavy atoms, and all the other non-hydrogen atoms were located by difference Fourier syntheses. The α -carbons of one of the Et₄N⁺ ions were disordered and were refined over two positions (relative occupancies 0.35 and 0.65) with a common temperature factor. The lattice thf was found to be present in partial occupancy and disordered. It was refined to a total occupancy of 0.6 over two positions (0.3 each) with idealized bond metricals. Each thf molecule was refined in the bow tie conformation, but the molecules did not share atoms. Hydrogen atoms were placed at calculated positions but were not refined. The hydrogen atoms of the β -carbons of the disordered Et₄N⁺ were refined as ideally disordered methyl groups with the occupancies tied to the disordered α -atoms. All non-hydrogen atoms of the ordered part of the molecule were refined with anisotropic displacement factors. Refinement on *F*² (SHELXL-93)^{24b} of all reflections except those with very negative *F*² converged to wR2 = 0.1802 (with *I* > 2 σ (*I*)) and a conventional R1 of = 0.0836. *R* factors based on *F*² are statistically about twice as large as those based on *F*, and *R* factors based on all data are even larger. Selected final positional parameters of [Et₄N]₂[Ia] are presented in Table 2, with selected bond metricals given in Table 3.

Computational Details. All the computations were carried out with the extended Hückel method²⁵ using the modified Wolfsberg-Helmholz formula.²⁶ The atomic parameters utilized are taken from the literature.²⁷ In the calculated model, the three methyl groups of [Ia]²⁻ were replaced by hydrogen atoms (O–H = 0.96 Å). The molecular structure

- (19) Neumann, H.-P.; Ziegler, M. L. *J. Chem. Soc., Chem. Commun.* **1988**, 498.
 (20) Chisholm, M. H.; Huffman, J. C.; Koh, J. J. *Polyhedron* **1989**, *8*, 127–128.
 (21) Shieh, M.; Mia, F.-D.; Peng, S.-M.; Lee, G.-H. *Inorg. Chem.* **1993**, *32*, 2785–2788.

- (22) *International Tables for X-ray Crystallography*; Kynoch: Birmingham, England, 1974; Vol. 4, pp 99–101, 149–150.
 (23) *TEXSAN: Single Crystal Structure Analysis Software*, v. 5.0; Molecular Structure Corp.: Woodlands, TX, 1989.
 (24) (a) Sheldrick, G. M. In *Crystallographic Computing 3*; Sheldrick, G. M., Kruger, C., Goddard, R., Eds.; Oxford University Press: Oxford, England, 1985; pp 175–189. (b) Sheldrick, G. M. In preparation for *J. Appl. Crystallogr.*
 (25) (a) Hoffmann, R. *J. Chem. Phys.* **1963**, *39*, 1397–1412. (b) Hoffmann, R.; Lipscomb, W. N. *J. Chem. Phys.* **1962**, *36*, 2179–2189.
 (26) Ammeter, J. H.; Bürgi, H.-B.; Thibeault, J. C.; Hoffmann, R. *J. Am. Chem. Soc.* **1978**, *100*, 3686–3692.
 (27) (a) Summerville, R. H.; Hoffmann, R. *J. Am. Chem. Soc.* **1976**, *98*, 7240–7254. (b) Underwood, D.; Nowak, M.; Hoffmann, R. *Inorg. Chem.* **1985**, *24*, 2095.

Table 2. Atomic Coordinates ($\times 10^4$) for the Non-Hydrogen Atoms and Equivalent Isotropic Displacement Parameters ($\text{\AA}^2 \times 10^3$) of the Anionic Part of $[\text{Et}_4\text{N}]_2[(\text{OC})_5\text{MoAsMo}_3(\text{CO})_9(\mu_3\text{-OMe})_3\text{Mo}(\text{CO})_3]$

atom	x	y	z	$U(\text{eq})^a$
Mo(1)	1015(2)	8760(1)	5864(1)	38(1)
Mo(2)	-2(2)	7985(1)	6878(1)	39(1)
Mo(3)	-1482(2)	8729(1)	5943(1)	39(1)
Mo(4)	48(2)	9285(1)	7501(1)	43(1)
Mo(5)	-381(2)	7331(1)	4400(1)	44(1)
As(1)	-262(2)	8004(1)	5464(1)	37(1)
O(1)	-199(10)	9303(4)	6270(6)	30(3)
O(2)	1102(10)	8659(5)	7067(7)	42(4)
O(3)	-1128(10)	8621(5)	7127(7)	41(3)
O(11)	719(14)	8970(6)	4191(8)	68(5)
O(12)	2864(14)	7974(7)	5489(9)	74(5)
O(13)	2973(19)	9533(9)	5612(13)	116(9)
O(21)	1912(14)	7207(7)	6663(10)	75(5)
O(22)	-1723(15)	7092(8)	6668(10)	80(6)
O(23)	289(19)	7452(8)	8441(10)	106(8)
O(31)	-3322(15)	7895(7)	5605(10)	79(6)
O(32)	-3603(17)	9441(9)	5968(11)	109(8)
O(33)	-1873(15)	9062(7)	4304(9)	79(6)
O(41)	-1650(14)	10106(7)	7930(9)	71(5)
O(42)	1864(14)	10120(7)	7781(11)	80(6)
O(43)	436(19)	9119(8)	9163(10)	101(7)
O(51)	-2518(17)	6786(7)	4952(11)	92(7)
O(52)	-2085(17)	8019(8)	3409(11)	96(7)
O(53)	-349(17)	6522(8)	3132(10)	92(7)
O(54)	1730(16)	7803(7)	3704(11)	89(6)
O(55)	1188(17)	6546(8)	5302(12)	101(7)
C(1)	-328(20)	9812(8)	5975(12)	56(6)
C(2)	2161(17)	8570(8)	7456(11)	47(6)
C(3)	-2018(20)	8515(9)	7611(13)	67(7)
C(11)	812(17)	8896(8)	4808(13)	42(5)
C(12)	2158(20)	8252(10)	5646(12)	53(6)
C(13)	2225(23)	9256(13)	5757(15)	79(9)
C(21)	1165(20)	7485(8)	6697(12)	47(6)
C(22)	-1094(20)	7428(10)	6722(13)	55(6)
C(23)	211(21)	7671(11)	7892(14)	68(7)
C(31)	-2627(20)	8199(9)	5760(12)	49(6)
C(32)	-2790(21)	9171(10)	6003(12)	60(7)
C(33)	-1685(16)	8926(9)	4897(13)	45(6)
C(41)	-992(21)	9788(10)	7736(13)	57(7)
C(42)	1166(19)	9795(10)	7663(11)	49(6)
C(43)	256(21)	9176(10)	8512(13)	65(8)
C(51)	-1758(22)	6994(10)	4783(14)	64(7)
C(52)	-1468(22)	7783(10)	3751(16)	68(8)
C(53)	-395(20)	6808(11)	3596(14)	63(7)
C(54)	953(21)	7657(9)	3949(14)	56(7)
C(55)	625(20)	6842(9)	4999(13)	57(7)

^a One-third of the trace of the orthogonalized U_{ij} tensor.

of $[\text{Ia}]^{2-}$ was averaged so that the symmetry of the $(\text{CO})_3\text{Mo}(\text{OH})_3\text{Mo}_3(\text{CO})_9\text{As}$ fragment was C_{3v} . Because the $\text{Mo}(\text{CO})_5$ fragment attached to the As atom has no C_3 axis, the real symmetry group of the whole molecule is at most C_s . However, the symmetry of the levels associated to the $[\text{Mo}]_3$ core can be treated almost rigorously within the C_{3v} group. Calculations were also performed on isoelectronic models obtained by removal or replacement of the $\text{Mo}(\text{CO})_5$ substituent by a proton ($\text{As-H} = 1.52 \text{ \AA}$). In all cases, the results were very similar.

Results

Reaction of NaAsO_2 and $\text{Mo}(\text{CO})_6$ in refluxing methanol yields cleanly $[\text{Ia}]^{2-}$, whereas the same reaction in ethanol yields $[\text{Ib}]^{2-}$. The proton NMR spectra for $[\text{Ia}]^{2-}$ and $[\text{Ib}]^{2-}$ show only one alkoxy signal, and the carbonyl regions for both compounds show the expected pattern for five different carbonyl environments at approximately the same chemical shifts, consistent with the idealized local symmetries of the metal carbonyl fragments of $[\text{I}]^{2-}$. The IR spectrum in the carbonyl region is complex, as expected for the presence of one $\text{Mo}(\text{CO})_5$ and two different $\text{Mo}(\text{CO})_3$ environments. Positive ion

Table 3. Selected Bond Distances (\AA) and Angles (deg) for $[\text{Et}_4\text{N}]_2[(\text{OC})_5\text{MoAsMo}_3(\text{CO})_9(\mu_3\text{-OMe})_3\text{Mo}(\text{CO})_3]$

Mo(1)–Mo(2)	3.037(3)	Mo(1)–Mo(3)	3.022(3)
Mo(2)–Mo(3)	3.048(3)	Mo(1)–As(1)	2.553(3)
Mo(2)–As(1)	2.570(3)	Mo(3)–As(1)	2.570(3)
Mo(5)–As(1)	2.593(3)	Mo(1)–O(1)	2.191(12)
Mo(1)–O(2)	2.200(13)	Mo(2)–O(3)	2.196(13)
Mo(2)–O(2)	2.197(14)	Mo(3)–O(1)	2.187(12)
Mo(4)–O(2)	2.233(13)	Mo(4)–O(1)	2.239(11)
Mo(4)–O(3)	2.291(13)	Mo–C range	1.87–2.03
O(1)–Mo(1)–O(2)	74.0(4)	O(1)–Mo(1)–As(1)	100.4(3)
O(2)–Mo(1)–As(1)	100.2(4)	O(1)–Mo(1)–Mo(3)	46.3(3)
O(2)–Mo(1)–Mo(3)	85.6(3)	As(1)–Mo(1)–Mo(3)	54.11(7)
O(1)–Mo(1)–Mo(2)	84.6(3)	O(2)–Mo(1)–Mo(2)	46.3(4)
As(1)–Mo(1)–Mo(2)	53.90(7)	Mo(3)–Mo(1)–Mo(2)	60.41(6)
O(3)–Mo(2)–O(2)	75.8(5)	O(3)–Mo(2)–As(1)	99.3(4)
O(2)–Mo(2)–As(1)	99.8(3)	O(3)–Mo(2)–Mo(1)	85.3(3)
O(2)–Mo(2)–Mo(1)	46.4(3)	As(1)–Mo(2)–Mo(1)	53.38(7)
O(3)–Mo(2)–Mo(3)	45.7(3)	O(2)–Mo(2)–Mo(3)	85.0(3)
As(1)–Mo(2)–Mo(3)	53.63(7)	Mo(1)–Mo(2)–Mo(3)	59.55(6)
O(3)–Mo(3)–O(1)	74.7(4)	O(3)–Mo(3)–As(1)	99.7(4)
O(1)–Mo(3)–As(1)	100.0(3)	O(3)–Mo(3)–Mo(1)	85.9(3)
O(1)–Mo(3)–Mo(1)	46.4(3)	As(1)–Mo(3)–Mo(1)	53.59(7)
O(3)–Mo(3)–Mo(2)	46.1(3)	O(1)–Mo(3)–Mo(2)	84.4(3)
As(1)–Mo(3)–Mo(2)	53.63(7)	Mo(1)–Mo(3)–Mo(2)	60.04(6)
O(2)–Mo(4)–O(1)	72.4(5)	O(2)–Mo(4)–O(3)	73.2(5)
O(1)–Mo(4)–O(3)	71.6(4)	Mo(1)–As(1)–Mo(3)	72.30(8)
Mo(1)–As(1)–Mo(2)	72.72(8)	Mo(3)–As(1)–Mo(2)	72.75(8)
Mo(1)–As(1)–Mo(5)	136.13(11)	Mo(3)–As(1)–Mo(5)	137.58(11)
Mo(2)–As(1)–Mo(5)	136.93(11)	Mo(3)–O(1)–Mo(1)	87.3(4)
Mo(3)–O(1)–Mo(4)	107.2(5)	Mo(1)–O(1)–Mo(4)	106.4(5)
Mo(2)–O(2)–Mo(1)	87.3(5)	Mo(2)–O(2)–Mo(4)	105.8(5)
Mo(1)–O(2)–Mo(4)	106.3(6)	Mo(3)–O(3)–Mo(2)	88.2(5)
Mo(3)–O(3)–Mo(4)	105.6(5)	Mo(2)–O(3)–Mo(4)	103.9(5)
Mo–C–O range	172–178		

electrospray mass spectrometry of $[\text{Et}_4\text{N}]_2[\text{Ia}]$ gave a signal appropriate for $\{[\text{Et}_4\text{N}]_3[\text{Ia}]\}^+$, and the theoretical isotope distribution matches the observed spectrum reasonably well (Figure 1). On the basis of similar IR and NMR spectra, elemental analysis, and mass spectroscopy, the structure of $[\text{Et}_4\text{N}]_2[\text{Ib}]$ is proposed to be essentially the same as that of $[\text{Et}_4\text{N}]_2[\text{Ia}]$. Unfortunately, no crystals suitable for crystallographic analysis have been obtained to date.

$[\text{Et}_4\text{N}]_2[\text{Ia}] \cdot 0.6\text{thf}$ crystallizes in space group $P2_1/n$, with one anion in the asymmetric unit and no crystallographically imposed symmetry. Figure 2 shows the anionic part of the structure. Crystallographic data collection and refinement parameters are given in Table 1, while selected bond metrics are provided in Table 3. The structure may be described as a Mo_3As tetrahedron, capped with three triply bridging methoxy ligands around the Mo_3 group. The methoxides are bonded to a $\text{Mo}(\text{CO})_3$ fragment. The As atom donates its external lone pair of electrons to a $\text{Mo}(\text{CO})_5$ fragment to complete the structure. The Mo–Mo distances average $3.04(1) \text{ \AA}$, and the As–Mo distances average $2.56(1) \text{ \AA}$. The O–Mo distances of the Mo_3 unit are on the order of 2.18 \AA , whereas the O–Mo distances to Mo(4) are somewhat longer, ranging from $2.23(1)$ to $2.28(1) \text{ \AA}$. The Mo–As–Mo angles average 72.7° . The bond metrics for the carbonyl ligands are all within values expected for terminally-bound CO.

Discussion

The reaction to give the title compound probably proceeds via the nucleophilic attack of AsO_2^- on a metal-bound CO to generate CO_2 and a Mo–As bond as has been established for the reaction of $\text{Fe}(\text{CO})_5$ with NaBiO_3 in MeOH .²⁸ A set of CO stretching bands (1913 , 1778 , and 1738 cm^{-1}) was observed

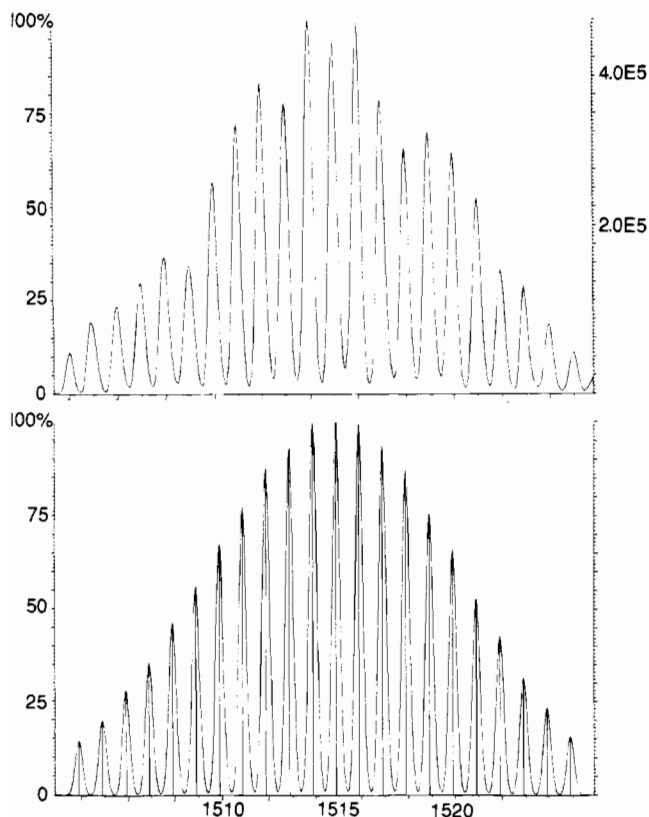


Figure 1. Observed (top) and calculated (bottom) mass distribution in the parent ion peak of $[\text{Et}_4\text{N}]_3[\text{II}]^+$.

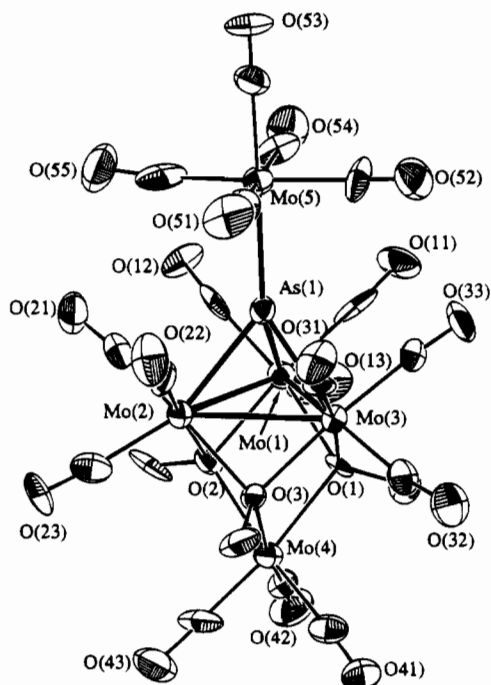


Figure 2. ORTEP drawing of the cluster anion found in $[\text{Et}_4\text{N}]_2[\text{IIa}]$. The ellipsoids are drawn at 50% probability. Carbon atoms are labeled according to the attached oxygen atoms, and hydrogen atoms have been omitted for clarity.

both for the crude reaction mixture and in a "blank" reaction of just $\text{Mo}(\text{CO})_6$ in MeOH, indicating that substitution of CO by MeOH may be occurring. It is unclear if this substitution precedes the nucleophilic attack of AsO_2^- or occurs concurrently. In contrast, neither $\text{Cr}(\text{CO})_6$ nor $\text{W}(\text{CO})_6$ reacted with NaAsO_2 in MeOH or EtOH, even after prolonged heating. While members of the same group often show consistent trends in

properties and similar reactivities, there are numerous exceptions. For example, the one-electron-reduction potentials of $\text{M}(\text{CO})_6$ in THF were found to be in the order $\text{Mo} < \text{W} < \text{Cr}$.²⁹

The Mo–As cluster compounds are air stable in the solid state, and crystals of both compounds left in air show no noticeable decomposition after several hours. The mass spectral data do not indicate the presence of any hydride ligands and demonstrate the usefulness of the electrospray technique for the characterization of highly charged anionic cluster compounds in the presence of tetraalkylammonium counterions. The compound is diamagnetic.

Structure of $[\text{Et}_4\text{N}]_2[\text{IIa}]$. The As–Mo bond lengths (2.56–(1) Å) are slightly longer than those found in both open and closed $\text{As}(\text{ML}_n)_3$ compounds such as $\{\text{CpMo}(\text{CO})_2\}_2\text{As}\{\text{MnCp}(\text{CO})_2\}_2$ (2.41 Å), $\{\text{MoCp}(\text{CO})_2\}_2\text{As}\{\text{Cr}(\text{CO})_5\}_2$ (2.36 Å),⁹ $\text{As}\{\text{MoCp}(\text{CO})_2\}_3$ (2.53 Å),¹¹ $\{\text{CpMo}\}_3(\mu\text{-O})_3\text{As}$ (2.45 Å), and $\{\text{MoCp}\}_3(\mu\text{-O})_2(\mu\text{-S})\text{As}$ (2.47 Å).¹⁹ This is more or less expected, since $[\text{IIa}]^{2-}$ is anionic and electron rich (*vide infra*). The As–Mo bond lengths are slightly shorter than those found in compounds containing polyarsenic fragments, $\{\text{MoCp}\}_2(\mu\text{-As}_5)$ (2.59(7) Å),¹⁰ $\text{MoCp}(\text{CO})_2\text{As}_3$ (2.673 Å),¹¹ and $\{\text{CpMo}(\text{CO})_2\}_2\{\text{As}_2\}_2$ (2.626(1) Å).¹² The Mo–Mo distances in the Mo_3 triangle are within the range of formal Mo–Mo single bonds as found in $[(\text{Cp})_3\text{Mo}_3(\text{CO})_6\text{S}]^+$ (3.085(21) Å), $[\text{HMo}(\text{CO})_3]_4^{4-}$ (3.11 (2) Å), $[\text{Cp}_2\text{Mo}_2(\text{CO})_6]$ (3.235 Å), $\text{Mo}_2(\text{CO})_{10}^{2-}$ (3.123 (7) Å), and $\text{RCCR}'\text{Mo}_2(\text{OR}'')_6$ (2.95–2.98 Å).³⁰ The compound is similar to $[\text{Et}_4\text{N}]_2[\text{II}]$, where the primary differences are longer Bi–Mo distances and ligation of As to an $\text{Mo}(\text{CO})_5$ group. These differences can be explained by the smaller size and greater basicity of As.

The electron-counting scheme chosen here is based upon the triangular Mo_3 unit. There are no Mo–Mo bonds from the Mo_3 triangle to Mo(4), and so the $[\text{Mo}(\text{CO})_3(\text{OMe})_3]^{3-}$ fragment is treated as a complex ligand attached to the cluster base. In this fragment, Mo(4) attains a standard 18e configuration via ligation by three 2e-donating carbonyl ligands and three 2e-donating alkoxides. These three bridging alkoxide ligands each function as 4e donors to the Mo_3As cluster core. The role of the As atom with regard to the four Mo atoms to which it is attached is conventional. It serves as a 2e donor to the external $\text{Mo}(\text{CO})_5$ group, leaving 3e for use in cluster bonding. The Mo_3 unit in this approach possesses a +1 charge and attains a 50e configuration which may be summarized as follows: 3e from As, 12e from the bridging alkoxides, 18e from the metal atoms plus 18e from the CO ligands less 1e for the positive charge. Other schemes based upon a neutral $\text{Mo}(\text{CO})_3(\text{OMe})_3$ fragment or other oxidation state distributions between the Mo_3 triangle and the As atom are possible but arrive at the same electron count. Fifty electrons is two more than predicted by the effective atomic number (EAN) rule which assumes 2-electron/2-center Mo–Mo bonds. Indeed, triangular M_3L_n complexes have generally $\text{VEC} = 48$,³¹ even when they form a tetrahedral closo cluster with a capping μ_3 -main group ligand.³² When $\text{VEC} = 50$, the usual arrangement satisfying the EAN rule is an open triangle with only two 2-electron metal–metal

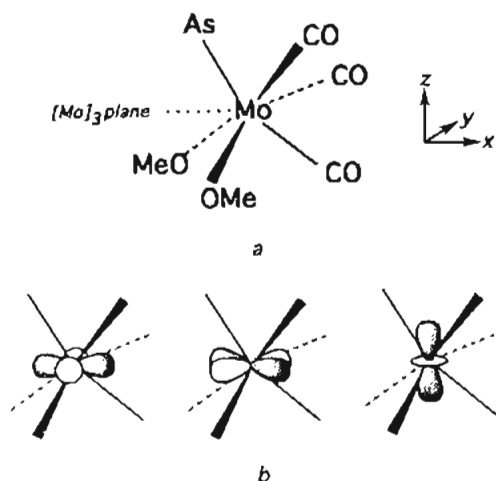
(29) Pickett, C. J.; Pletcher, D. *J. Chem. Soc., Dalton Trans.* **1975**, 879.

(30) Cotton, F. A.; Walton, R. A. In *Multiple Bonds between Metal Atoms*; Clarendon Press: Oxford, England, 1993. Adams, R. D.; Collins, D. M.; Cotton, F. A. *Inorg. Chem.* **1974**, *13*, 1086. T'suen, J.; Ellis, J. E. *J. Am. Chem. Soc.* **1983**, *105*, 6252–6258. Handy, L. B.; Ruff, J. K.; Dahl, L. E. *J. Am. Chem. Soc.* **1970**, *92*, 7312. Curtis, M. D.; Butler, W. M. *J. Chem. Soc., Chem. Commun.* **1980**, 998–1000.

(31) See for example: Schilling, B. E. R.; Hoffmann, R. *J. Am. Chem. Soc.* **1979**, *101*, 3456–3467 and references therein.

(32) Wade, K. *Inorg. Nucl. Chem. Lett.* **1978**, *14*, 71.

Chart 1



bonds.³³ Nevertheless, a few equilateral triangular $[M_3]$ clusters having a VEC = 50 have been reported.³⁴ They all exhibit rather long M–M bond distances, in agreement with their electron excess. On the other hand, if each Mo atom in the triangle attained an 18e configuration with *no* M–M bonding, a total of 54e would be expected. It is noteworthy that the related clusters $[Ia]^{2-}$ and $[II]^{2-}$ are the only examples of such trinuclear electron-rich systems in early-transition-metal chemistry.

Theoretical Study

Qualitative Approach. Each of the metal atoms of the $[Mo_3]$ core is bonded to six ligands in a distorted octahedral environment. The $[Mo_3]$ plane bisects each of these octahedra in the way depicted in Chart 1a. The Mo–Mo bonding within the triangle can then be conceptually analyzed as resulting from the interaction of three “ MoL_6 ” units. Although distorted, the octahedral environment of one metal atom splits its d orbitals into the usual “ e_g ” and “ t_{2g} ” groups. The levels of “ e_g ” pseudosymmetry are significantly metal–ligand antibonding, lie at high energy, and are vacant. The “ t_{2g} ” orbitals are mainly nonbonding and lie at lower energy. They are represented in Chart 1b. In our local coordinate system, they derive principally from the $x^2 - y^2$, xy , and z^2 atomic orbitals (AOs). They are the frontier molecular orbital (FMO) set of the “ MoL_6 ” subunits.

Within the strong C_{3v} pseudosymmetry of cluster $[Ia]^{2-}$, the $x^2 - y^2$ FMOs of the three metal atoms combine to give a set of a_1 (Mo–Mo bonding) + e (Mo–Mo antibonding) MOs. The three xy FMOs combine to form an orbital set of e (Mo–Mo bonding) + a_2 (Mo–Mo antibonding) symmetry. The z^2 FMOs, poorly localized in the Mo_3 plane, overlap weakly and lead to more or less nonbonding combinations of $a_1 + e$ symmetry. To summarize, the “ t_{2g} ” system leads to three mainly bonding orbitals ($a_1 + e$), three mainly nonbonding orbitals ($a_1 + e$), and three antibonding orbitals ($a_2 + e$), allowing for some mixing between combinations of the same symmetry. Assuming that all the metal–ligand interactions are 2-electron/2-center bonds, seven of these MOs are occupied, which means that one

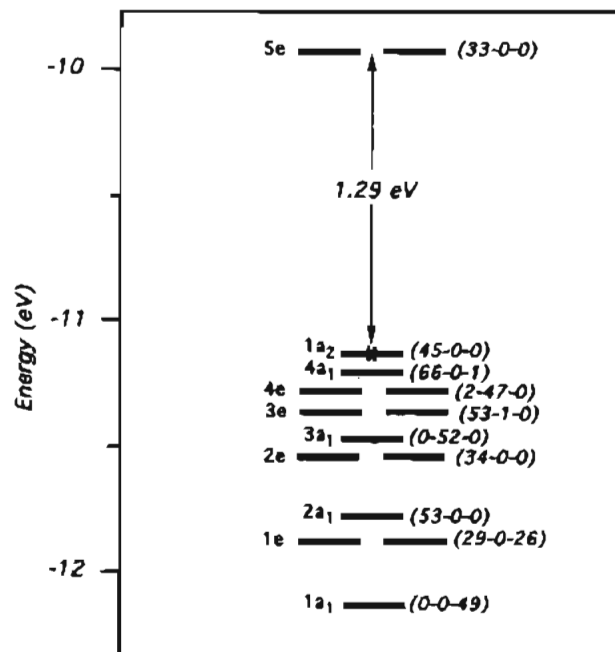


Figure 3. Molecular orbital diagram for the model $[Mo_4(\mu_3-AsMo(CO)_5)(CO)_{12}(\mu-OH)_3]$. MOs are labeled in the C_{3v} symmetry group. Numbers in parentheses indicate the percentage metal character for the triangle $[Mo_3]$, Mo(4), and Mo(5), respectively.

antibonding level is occupied by the extra electron pair. Since the three Mo–Mo bonds are equivalent, it is likely that these two electrons are located in the antibonding a_2 level. Either a Jahn–Teller distortion or a triplet state, which is not observed, would be expected if they were located in the antibonding e level. A similar electron distribution has been proposed for related electron-rich trinuclear triangular systems.^{34b,d}

Electronic Structure of $[Ia]^{2-}$. Extended Hückel calculations have been carried out on an idealized model of $[Ia]^{2-}$ in which the methyl groups were replaced by hydrogen atoms and with a symmetry very close to C_{3v} (see the Experimental Section). The corresponding MO diagram, shown in Figure 3, is in full agreement with the electron configuration predicted from the qualitative analysis. The upper group of occupied levels is made of thirteen metallic MOs. Seven of them are localized on the $[Mo_3]$ core (two of a_1 symmetry ($2a_1$ and $4a_1$), two of e symmetry ($2e$ and $3e$), and one a_2 symmetry ($1a_2$), as expected from above). Among the six remaining ones, three ($3a_1$ and $4e$) are localized mainly on Mo(4) and three ($1a_1$ and $1e$) on Mo(5). They correspond to the “ t_{2g} ” MOs expected for octahedrally coordinated metal atoms.

The HOMO of $[Ia]^{2-}$, plotted in Figure 4, is the $[Mo_3]$ antibonding $1a_2$ combination. The computed Mo–Mo overlap population in this level is -0.018 . We cannot identify the bonding electron pair in a single a_1 level. The a_1 bonding character is actually distributed over the two $[Mo_3]$ $2a_1$ and $4a_1$ MOs (the corresponding Mo–Mo overlap populations are $+0.020$ and $+0.028$, respectively). From the plot given in Figure 4, one can see that $2a_1$ possesses a large $x^2 - y^2$ character, whereas $4a_1$ is predominantly made of z^2 AOs, with some 5s admixture. The total Mo–Mo overlap population ($+0.059$) indicates rather weak metal–metal bonding. Consistent with the structural parameters, there is essentially no Mo···Mo interaction between the $[Mo_3]$ core and Mo(4) (the corresponding Mo···Mo overlap population is -0.004).

The computed HOMO/LUMO gap is large (1.29 eV), in agreement with the stability and diamagnetism of $[Ia]^{2-}$. As expected from above, the 5e LUMOs are Mo–Mo antibonding.

(33) See for example: Albers, M. O.; Robinson, D. J.; Coville, N. J. *Coord. Chem. Rev.* **1986**, *69*, 127 and references therein.

(34) (a) Cherkas, A. A.; Taylor, N. J.; Carty, A. J. *J. Chem. Soc., Chem. Commun.* **1990**, 385–387. (b) Mealli, C. *J. Am. Chem. Soc.* **1990**, *112*, 2245–2253. (c) Cabeza, J. A.; Lahoz, F. J.; Martín, A. *Organometallics* **1992**, *11*, 2754–2756. (d) Lugan, N.; Fabre, P.-L.; de Montauzon, D.; Lavigne, G.; Bonnet, J.-J.; Saillard, J.-Y.; Halet, J.-F. *Inorg. Chem.* **1993**, *32*, 1363–1369. (e) Corrigan, J. F.; Doherty, S.; Taylor, N. J.; Carty, A. J. *J. Organomet. Chem.* **1994**, *462*, C24–C26.

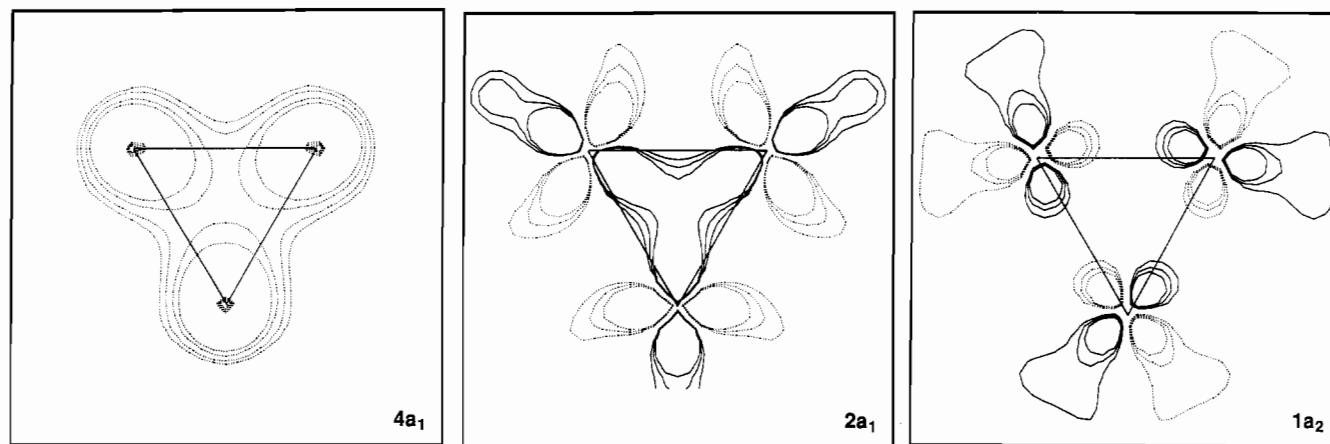


Figure 4. Contour maps in the $[\text{Mo}_3]$ plane for the $2a_1$, $4a_1$, and $1a_2$ MOs of the $[\text{Mo}_4(\mu_3\text{-AsMo}(\text{CO})_5)(\text{CO})_{12}(\mu\text{-OH})_3]$ model.

The Mo–Mo overlap population in each of these orbitals is -0.018 , a value equal to the one corresponding to the $1a_2$ HOMO. The question which arises then is the following: Why is the $5e$ level so much higher in energy than that of the $1a_2$ orbital if they represent similar Mo–Mo antibonding character? The answer lies in their different ligand character. As we can see in Figure 4, the $1a_2$ HOMO presents a significant Mo–CO bonding character, due to some in-phase mixing of π^*_{CO} orbitals into this d level. On the other hand, the $5e$ LUMOs are destabilized by low-lying ligand levels of the same symmetry deriving from the oxygen p lone pairs and from the arsenic 4p AOs. This metal–ligand antibonding mixing induces in turn, a large admixture of the Mo z^2 AOs in the $5e$ level, leading to the increase of its metal–ligand antibonding character. Clearly, the nature of the metal–ligand interactions is the main factor responsible for the HOMO ($1a_2$)/LUMO ($5e$) splitting. This mixing of ligand orbitals in levels of “ t_{2g} ” parentage is favored by the distortion of the Mo ligand shell away from the ideal octahedral symmetry. This distortion induces some additional stabilization of occupied “ t_{2g} ” MOs by high-lying vacant “ e_g ” levels.

Conclusion

Although bearing an excess of two electrons with respect to the triangular arrangement of the $[\text{Mo}_3]$ core, compound $[\mathbf{1a}]^{2-}$ does not present any Jahn–Teller instability, which would lead to the formation of an open $[\text{Mo}_3]$ triangle. It turns out that the extra electron pair does not occupy a degenerate e level but is housed in an a_2 orbital equally delocalized over the three metal atoms. For this electron configuration, a large HOMO/LUMO gap is computed, principally resulting from the different nature (bonding or antibonding) of the metal–ligand interactions. Although significant, the Mo–Mo bonding in the triangle is

weak, the stability of this C_{3v} architecture being partly due to the bridging ligands.

Is it possible to oxidize $[\mathbf{I}]^{2-}$ and to generate a 48-electron species with three two-electron localized Mo–Mo bonds? This process might involve the partial or complete depopulation of the $1a_2$ HOMO, leading to some shortening of the Mo–Mo separations, without changing the molecular framework tremendously. If this soft structural rearrangement was able to induce a significant destabilization of $1a_2$, it should be possible to isolate 48-electron neutral compounds of the type $\text{Mo}_4(\mu_3\text{-EMo}(\text{CO})_5)(\text{CO})_{12}(\mu\text{-OR})_3$ or $\text{Mo}_4(\mu_3\text{-E})(\text{CO})_{12}(\mu\text{-OR})_3$ with $\text{E} = \text{P, As, Sb, or Bi}$. However, the formation upon oxidation of some bonding between Mo(4) and the $[\text{Mo}_3]$ core cannot fully be ruled out. Indeed, the corresponding nonbonding contacts in $[\mathbf{1a}]^{2-}$ are rather short (about 3.55 Å). One orbital of the d block ($3a_1$), which can be identified as the z^2 level of Mo(4), could form an antibonding combination with the $[\text{Mo}_3]$ $4a_1$ level upon shortening of the Mo(4)– $[\text{Mo}_3]$ contacts. This orbital could consequently be depopulated in the oxidized species.

Acknowledgment. This work was assisted by a grant from an NSF/CNRS exchange program. B.Z., J.-F.H., and J.-Y.S. are grateful to Franco-Algerian Research Program 90MDU136 and K.H.W and J.W.v.H. thank the Robert A. Welch Foundation and the National Science Foundation (Grant CHE-9408613) for support. VG is acknowledged for providing mass spectral data.

Supporting Information Available: Tables of all atomic coordinates, including those for the hydrogen atoms, anisotropic displacement factors, full crystallographic data collection parameters, and bond distances and angles for $[\text{Eu}_2\text{N}]_2[\mathbf{1a}]\cdot 0.6\text{thf}$ (10 pages). Ordering information is given on any current masthead page.

IC9411817